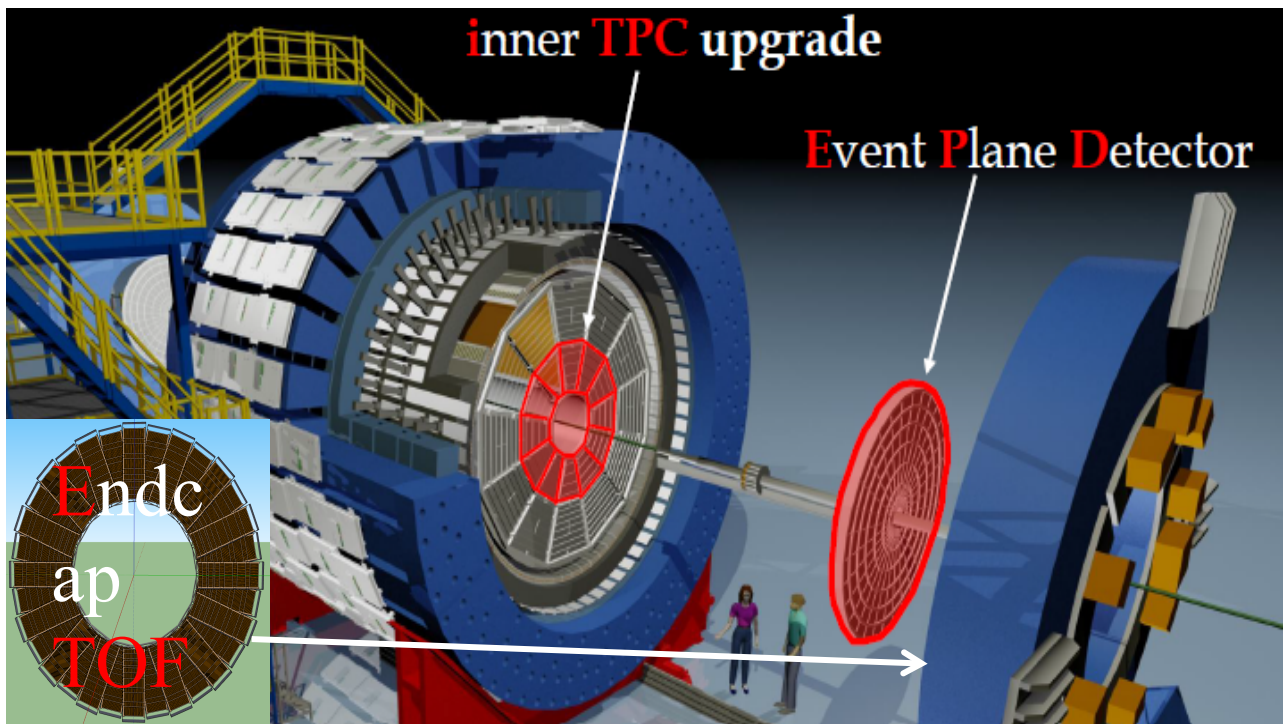


Highlights of the STAR midrapidity Physics Program after 2020



May 2017

1	EXECUTIVE SUMMARY	5
2	THE STAR DETECTOR IN 2021+	6
3	PHYSICS HIGHLIGHTS AT MID RAPIDITY IN 2021+	7
3.1	PHYSICS OPPORTUNITIES WITH (UN)POLARIZED PROTON-PROTON COLLISIONS	7
3.2	PHYSICS OPPORTUNITIES WITH (UN)POLARIZED PROTON-NUCLEUS COLLISIONS	11
3.3	PHYSICS OPPORTUNITIES WITH NUCLEUS-NUCLEUS COLLISIONS	15
3.3.1	DI-ELECTRON MASS SPECTRUM MEASUREMENT IN 2020+	15
3.3.2	HYPERTRITON LIFETIME MEASUREMENT IN 2020+	17
3.4	PHYSICS OPPORTUNITIES WITH DIFFRACTIVE AND ULTRA-PERIPHERAL COLLISIONS IN PP, PA AND AA	18
4	BIBLIOGRAPHY	19

1 Executive Summary

Since its inception, the hallmark of the STAR detector has been full acceptance mid-rapidity measurements with excellent particle identification capabilities. Upgrades that are currently underway to maximize the physics output from Beam Energy Scan phase II will substantially enhance STAR's already excellent capabilities. These upgrades will enable STAR to continue its unique, ground-breaking mid-rapidity science program in the period following BES-II.

In this document, the STAR collaboration presents a science driven program for future polarized p+p, p+A A+A beam operations at RHIC. A suite of unique measurements that can only be made with a p+p, p+A, and Au+Au collider are discussed. **The physics program described in this document complements the program discussed in the STAR forward upgrade proposal [1].** The program is designed to capitalize on STAR's existing resources, which include a proven multi-purpose detector, established calibration techniques and highly developed software infrastructure and are a natural extension of the current STAR physics program. The programs outlined here and in the forward upgrade proposal are an essential step towards the completion of the RHIC mission and will provide a natural transition to the highly anticipated electron-ion collider program.

The key physics opportunities envisioned address three broad areas of interest within the cold QCD community in the years following the BES-II. These programs will shed light on the dynamics of low and high x partons in cold nuclear matter (CNM) and how the fragmentation and hadronization of these partons is modified through interactions within the CNM and experiments to study the 2+1d spatial and momentum structure of protons and nuclei. These measurements will provide critical new insights into the QCD structure of nucleons and nuclei in the near term, as well as the high precision data that will be essential to enable rigorous universality tests when combined with future results from the EIC. In A+A collisions measurements with unprecedented precision using deep penetrating probes as leptons and photons will enable us to probe the whole evolution of the collision. In addition, significantly improved hypertriton lifetime measurements may have important implications on astrophysics.

All projections and physics discussions are based on the following already planned data taking periods during the sPHENIX running periods in 2022 and 2023:

1. **2022:** 20 weeks of Au+Au at $\sqrt{s} = 200$ GeV
2. **2023:** 8 weeks transversely polarized p+p at $\sqrt{s} = 200$ GeV
3. **2023:** 8 weeks each of transversely polarized p+Au and p+Al at $\sqrt{s} = 200$ GeV

In addition, a 20 week $\sqrt{s} = 500$ GeV polarized p+p run, split between transverse and longitudinal polarized running is proposed based on its merits for the overall physics program laid out in this document. This run could be scheduled in 2021, for which currently no dedicated physics program is assigned. It is especially noted none of the data taking periods proposed would result in any extra time delay to an eRHIC construction. **It is also noted that this high impact and cost-effective physics program can be executed even in challenging financial times as all the needed detector capabilities are already existing in STAR.**

2 The STAR detector in 2021+

STAR has three upgrades underway to maximize the physics output from BES-II – the Event Plane Detector (EPD), the inner Time Projection Chamber (iTPC), and the endcap Time of Flight (eTOF) – shown in Figure 2-1. The current status of the three upgrades is described in [2].

The EPD will replace the BBC as a minimum-bias trigger detector and will provide forward measurements of the event plane and centrality. The iTPC will increase the acceptance of the TPC from $|\eta| < 1$ to $|\eta| < 1.5$, improve the dE/dx resolution, and allow tracks to be reconstructed down to $p_T \sim 60$ MeV/c. The eTOF will extend STAR's PID capabilities at forward rapidities. The EPD will be completed in time for Run 18. The iTPC and eTOF will be completed in time for Run 19. Although these three upgrades are being constructed with BES-II physics in mind, they will also bring STAR powerful new detection capabilities for unique measurements in p+p, p+A, and full-energy Au+Au collisions. Thus, it will be essential for STAR to continue running beyond the BES-II era in order to fully amortize the upgrade investments that are underway now.

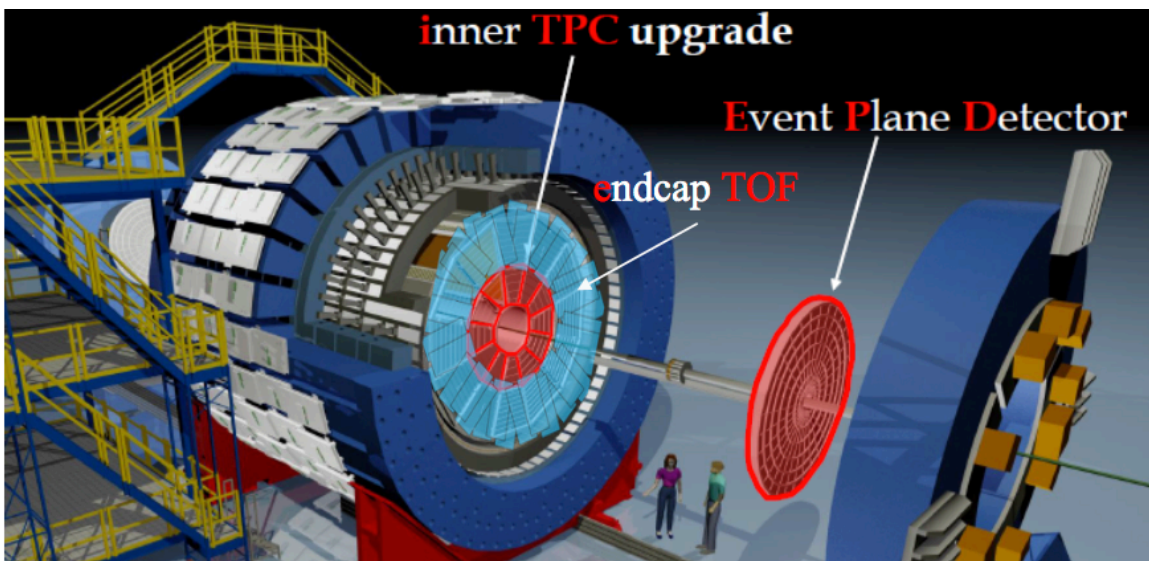


Figure 2-1: A view of the STAR detector with the BES-II upgrades highlighted. The EPD and iTPC are symmetric in STAR. The eTOF is only on the east side, opposite the EEMC, FMS, and future FCS-FTS forward upgrade.

The EPD is a new, dedicated event plane, centrality, and trigger detector. It will consist of two scintillator arrays covering the pseudorapidity region $2.1 < |\eta| < 5.1$ at both ends of STAR. Each array will include 372 scintillator tiles, arranged with 24 azimuthal tiles in each of 15 eta rings, plus 12 azimuthal tiles in a 16th (most forward) eta ring. This represents approximately 10 times the granularity of the BBC that it will replace. It will provide precision measurements of the event plane and centrality that are well-separated in pseudorapidity from the TPC. This will dramatically reduce non-flow systematics in v_n measurements and auto-correlations in fluctuation measurements.

The iTPC is an upgrade to the inner sectors of the TPC to increase the segmentation on the inner pad planes. At present, only $\sim 20\%$ of the area of the inner pad planes is active. The full area will be active with the iTPC. This will extend the TPC acceptance for good track measurements from $|\eta| < 1$ to $|\eta| < 1.5$ and improve the dE/dx resolution by up to 25%. In p+p collisions, the increased η acceptance will extend the x coverage of Collins effect and interference fragmentation function measurements. In Au+Au collisions, the increased η acceptance will, for example, enable correlation measurements, including those investigating longitudinal de-correlations, to examine a 50% wider pseudorapidity window. The improved dE/dx resolution will enhance essentially all

STAR identified particle measurements. Two examples include identified particle fragmentation functions in jets in p+p and p+A collisions, both unpolarized and polarized, and low- and intermediate-mass di-electron measurements in Au+Au collisions.

The eTOF will provide time-of-flight measurements for particle identification in the region $-1.6 < \eta < -1.1$, complementing the existing Barrel TOF measurements in the region $|\eta| < 0.9$. Figure 2-2 shows the particle identification capabilities of the combined iTPC and eTOF. They will, for example, substantially extend the reach of di-electron measurements in Au+Au collisions. The eTOF is joint project between STAR and CBM that provides important new physics capabilities to STAR, while providing our CBM colleagues the opportunity to operate $\sim 10\%$ of their ultimate time-of-flight system in realistic experimental conditions. The current MOU between STAR and CBM states that the eTOF will remain at STAR through the end of BES-II. Whether it remains after BES-II will depend on the physics programs and needs of STAR and CBM at that time.

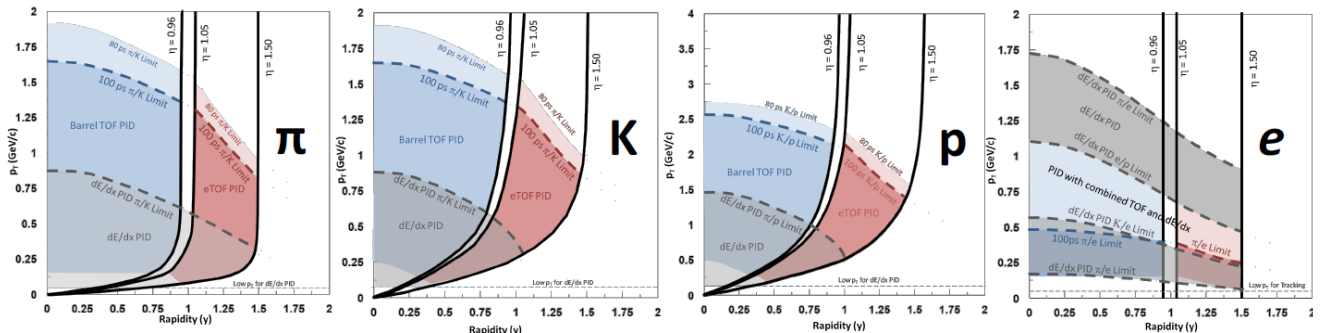


Figure 2-2: Acceptance and PID capabilities for π , K , proton, and electrons at low- and intermediate p_T with the combination of iTPC and eTOF.

3 Physics Highlights at mid rapidity in 2021+

3.1 Physics opportunities with (un)polarized proton-proton collisions

The enhanced tracking and particle identification capabilities provided by the iTPC upgrade will allow STAR to increase the statistical power and kinematic reach of several flagship measurements. In the case of $\sqrt{s} = 200$ GeV collisions STAR would prioritize the Collins and Interference Fragmentation Function (IFF) transverse spin asymmetry (A_{UT}) measurements. The Collins measurement requires the reconstruction of the angular distribution of charged pions around the axis of a jet, while the IFF requires the reconstruction of di-hadron pairs. Note that both channels rely on particle identification and measurements to date are restricted to the current STAR TPC acceptance ($|\eta| < 1$).

Both the Collins and IFF asymmetries are sensitive to the transversity distribution [3,4,5], $\delta q(x)$, which can be interpreted as the net transverse polarization of quarks within a transversely polarized proton[6]. A complete picture of nucleon spin structure at leading twist must consider not only unpolarized and helicity distributions, but also those involving transverse polarization, such as the transversity distribution [6,7,8]. It is also noted that the difference between the helicity distributions and the transversity distributions for quarks and antiquarks provides a direct, x -dependent, connection of nonzero orbital angular momentum components in the wave function of the proton⁹. Recently, the measurement of transversity has received renewed interest to access the tensor charge of the nucleon, defined as the integral over the valence quark transversity: $\int_0^1 (\delta q^a(x) - \delta \bar{q}^a(x)) dx = \delta q^a$ [6,10]. Measuring the tensor charge is important for two reasons: It can be calculated on the lattice with comparatively high precision, and due to the valence nature of transversity, it is one of the few

quantities that allow us to compare experimental results on the spin structure of the nucleon to ab-initio QCD calculations. The second reason is that the tensor charge describes the sensitivity of observables in low energy hadronic reactions to beyond the standard model (BSM) physics processes with tensor couplings to hadrons. Examples are experiments with ultra-cold neutrons and nuclei.

Transversity is difficult to access due to its chiral-odd nature, requiring the coupling of this distribution to another chiral-odd distribution. Semi-inclusive deep inelastic scattering (SIDIS) experiments have successfully probed transversity through two channels: asymmetric distributions of single pions, coupling transversity to the transverse-momentum-dependent (TMD) Collins fragmentation function [11], and azimuthally asymmetric distributions of di-hadrons, coupling transversity to the so-called “interference fragmentation function” [12] in the framework of collinear factorization. Taking advantage of universality and robust proofs of TMD factorization for SIDIS, recent results [13,14,15,16] have been combined with e^+e^- measurements isolating the Collins and IFFs [17,18] for the first global analyses to extract simultaneously the transversity distribution and polarized FF. In spite of this wealth of data, the kinematic reach of existing SIDIS experiments, where the range of Bjorken- x values does not reach above $x \sim 0.3$, limits the current extractions of transversity.

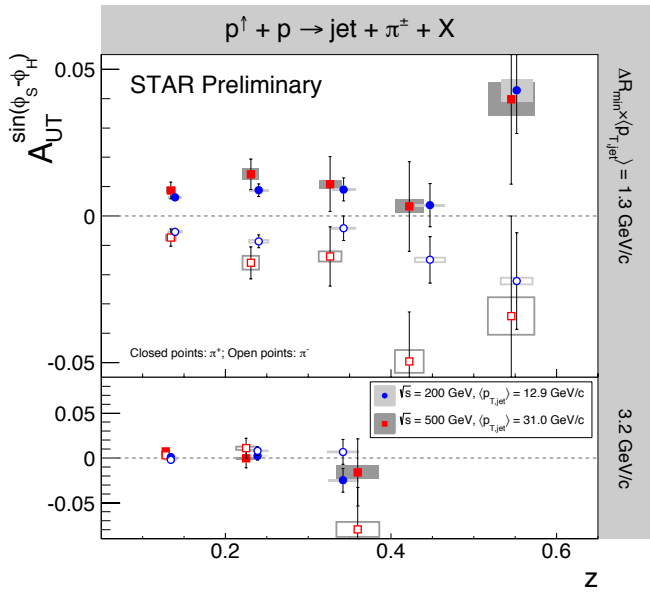


Figure 3-1: $A_{UT}^{\sin(\phi_s - \phi_h)}$ vs. z for charged pions in jets at $0 < \eta < 1$ from p+p collisions at $\sqrt{s} = 200$ GeV and 500 GeV by STAR. The $p_{T,jet}$ ranges have been chosen to sample the same parton x values for both beam energies. The angular cuts, characterized by the minimum distance of the charged pion from the jet thrust axis, have been chosen to sample the same j_T -values ($j_T \sim z \times \Delta R \times p_{T,jet}$). These data show for the first time a nonzero asymmetry in p+p collisions sensitive to transversity x Collins FF.

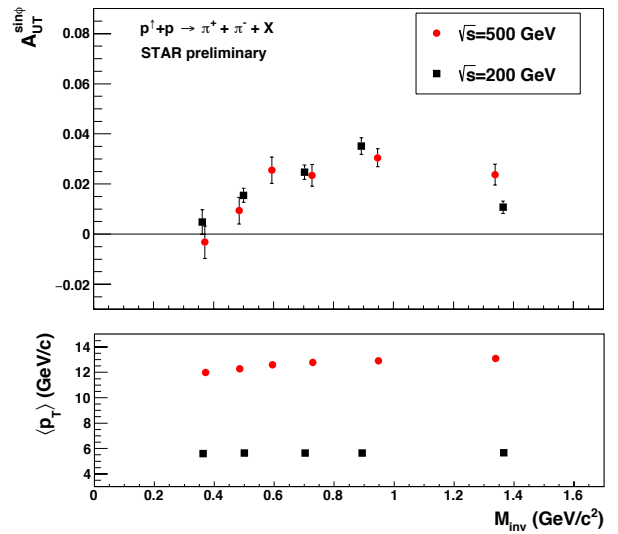


Figure 3-2: $A_{UT}^{\sin(\phi)}$ as a function of $M_{\pi^+\pi^-}$ (upper panel) and corresponding $p_{T(\pi^+\pi^-)}$ (lower panel). A clear enhancement of the signal around the ρ -mass region is observed both at $\sqrt{s} = 200$ GeV and 500 GeV by STAR for $-1 < \eta < 1$. The $p_{T(\pi^+\pi^-)}$ was chosen to sample the same x_T for $\sqrt{s} = 200$ GeV and 500 GeV.

Although large Collins and IFF asymmetries have been observed in SIDIS experiments for over a decade, the size and nature of these effects in hadronic collisions remained uncharted territory. STAR was the first experiment to demonstrate that significant mid-rapidity Collins and IFF asymmetries also exist in proton-proton collisions. Figure 3-1 and Figure 3-2 show the Collins and IFF A_{UT} at $\sqrt{s} = 200$ and 500 GeV center-of-mass energies. A comparison of the transversity signals extracted from the Collins and IFF measurements will explore questions about universality

and the size of factorization breaking effects. While the measurements of transversity through the Collins FF need TMD factorization to hold in p+p scattering, di-hadron asymmetries utilize collinear factorization. The first extraction of transversity from the STAR IFF data [19] has started (for details see Figure 14 in [20]). Thus, not only can more precise measurements of these effects in p+p improve our knowledge of transversity, such measurements are invaluable to test the longstanding theoretical questions, such as the magnitude of any existing TMD factorization breaking.

STAR's measurements also provide unique and invaluable information on TMD evolution. Comparisons of measurements at 200 and 500 GeV provide direct experimental constraints on evolution effects and the Collins FFs extracted from STAR data (e.g. Ref. [21]) can also be compared with extractions from SIDIS and e^+e^- data. Note that p+p collisions have a higher sensitivity to the d-quark transversity than SIDIS channels because there is no charge weighting in the hard scattering QCD $2 \rightarrow 2$ process in p+p collisions. This is a fundamental advantage of p+p collisions, as any SIDIS measurement of the d-quark transversity has to be on a bound system, i.e. He-3, which leads to nuclear corrections. The high scale we can reach in 500 GeV collisions at RHIC will also allow for the verification that previous SIDIS measurements at low scales in fact accessing the nucleon at leading twist. Figure 3-3 shows the $x-Q^2$ coverage spanned by the RHIC measurements compared to a future EIC, JLab-12, and the current SIDIS world data.

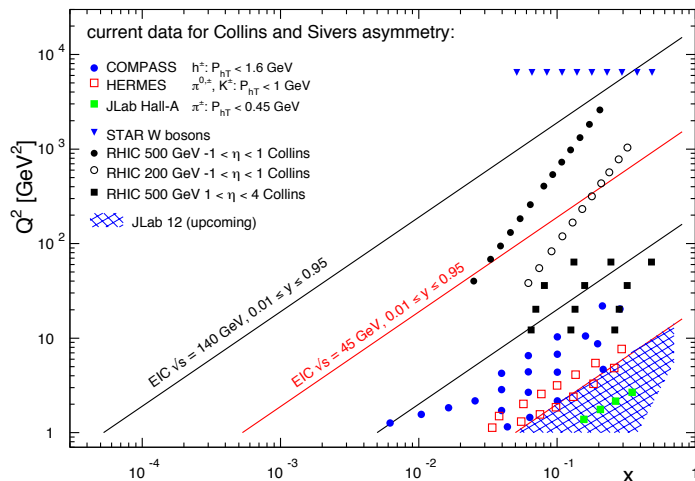


Figure 3-3 The $x-Q^2$ plane for data from the future EIC and Jlab-12 GeV as well as the current SIDIS data and the W-boson data from RHIC. All data are sensitive to the Siverts function and transversity times the Collins FF in the TMD formalism.

If the opportunity for a polarized p+p run at $\sqrt{s} = 500$ GeV should arise it would STAR would use the data to significantly improve the statistical power of both the Collins and IFF A_{UT} . Figure 3-4 (left) shows the expected uncertainties after the completion of the 2017 RHIC run. These error bars would be reduced by a factor of 2x for an additional 10 week run with 1.1 fb^{-1} recorded. The increase in center-of-mass energy generally shifts the accessible momentum fraction range to lower and higher x , providing new and stronger constraints on the functional form of the quark transversity distributions. Additional statistics at higher \sqrt{s} also facilitates more stringent tests of the TMD evolution and the size of factorization breaking effects in the Collins and Collins-like measurements.

Another fundamental advantage of p+p collisions is the ability to access gluons directly. While gluons cannot carry any transverse spin, there is a strong analogy between quark transversity and the linear polarization of gluons. Similarly, there exists an equivalent of the Collins fragmentation function for the fragmentation of linearly polarized gluons into unpolarized hadrons [22]. The linear polarization of gluons is a largely unexplored phenomenon, but it has been a focus of recent theoretical work, in particular due to the relevance of linearly polarized gluons in unpolarized hadrons for the p_T spectrum of the Higgs boson measured at the LHC. Polarized proton collisions with $\sqrt{s} = 500$ GeV at RHIC, in particular for asymmetric parton scattering if jets are

detected in the backward direction are an ideal place to study the linearly polarized gluon distribution in **polarized** protons (Note: that the distributions of linearly polarized gluons inside an unpolarized and a polarized proton provide independent information). A first measurement of the ‘‘Collins-like’’ effect for linearly polarized gluons has been done by STAR with data from Run-2011, providing constraints on this function for the first time. As with the Collins and the IFF measurement, the ‘‘Collins-like’’ channel will be extracted from the Run 17 $\sqrt{s} = 500$ GeV data with the statistical errors shown in Figure 3-4 (right), and these errors would be similarly reduced by a factor of 2x with an additional 1.1 fb^{-1} of data.

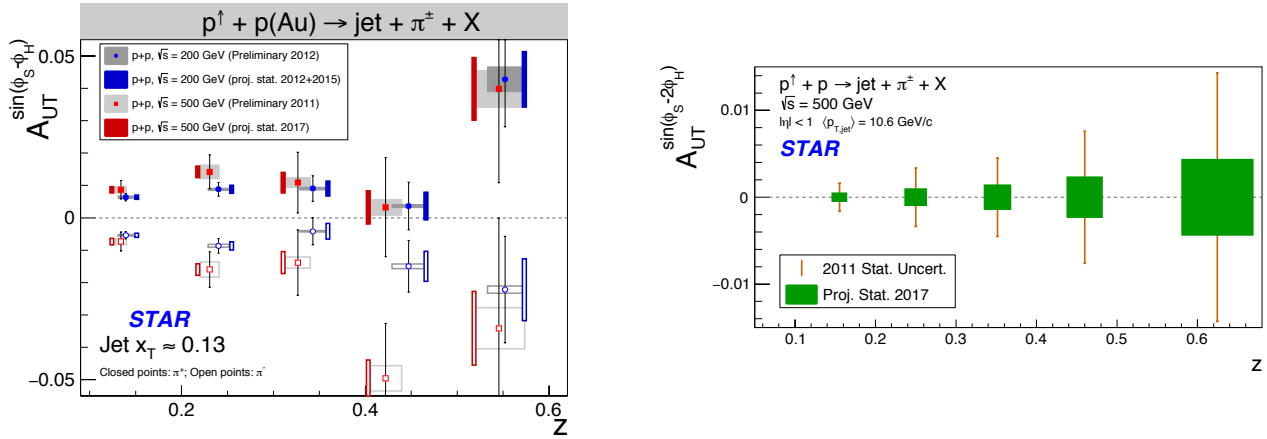


Figure 3-4: The statistical uncertainties for $A_{UT}^{\sin(\phi_s - \phi_h)}$ sensitive to the Collins effect and quark transversity (left) and $A_{UT}^{\sin(\phi_s - 2\phi_h)}$ sensitive to gluon linear polarization (right), as function of z for charged pions in jets at $0 < \eta < 1$ measured in STAR for transversely polarized p+p collisions at $\sqrt{s} = 200$ GeV (Run-2012 to Run-2015) and 500 GeV (Run-2011 to Run-2017), respectively.

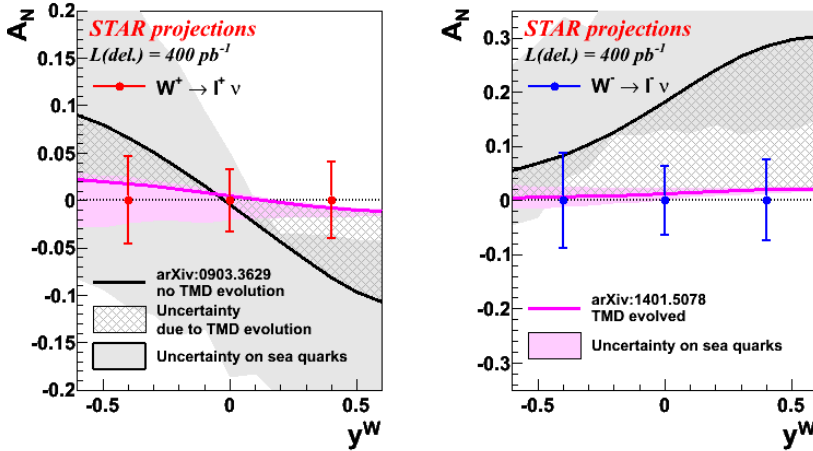


Figure 3-5: The projected uncertainties for transverse single-spin asymmetries of W^\pm and Z^0 bosons as functions of rapidity for a delivered integrated luminosity of 400 pb^{-1} and an average beam polarization of 55%. The solid light gray and pink bands represent the uncertainty on the KQ [23] and EIKV [24] known sea quark Sivvers function. The crosshatched dark grey region indicates the current uncertainty in the theoretical predictions due to TMD evolution.

Collisions at $\sqrt{s} = 500$ GeV would also allow STAR to continue their successful program to study the evolution and sign change of the Sivvers function in hadronic collisions. The improved tracking capabilities provided by the iTPC upgrade would allow the mid-rapidity $W^{+/-}$ and Z^0 A_N measurements to be pushed to larger $y^{W/Z}$, a regime where the asymmetries are expected to increase and the anti-quark Sivvers’ functions will remain largely unconstrained. Figure 3-5 demonstrates the expected precision of asymmetry measurements after data from the 2017 run is analyzed. In addition to extending the kinematic reach, an additional 10 weeks of beam time, $\sim 1.1 \text{ fb}^{-1}$ of integrated luminosity, would reduce the projected uncertainties by a factor of 2. This

experimental accuracy would significantly enhance the quantitative reach of testing the limits of factorization and universality in lepton-proton and proton-proton collisions.

The Sivers function, which encapsulates the correlation between the transverse momentum of the parton inside the proton to the transverse spin of the proton, is by definition a TMD observable. It is possible to connect this TMD observable to the analog twist-3 function via the Efremov-Teryaev-Qui-Sterman (ETQS) function [25]. A high luminosity run at $\sqrt{s} = 500$ GeV would provide the opportunity to make a high precision measurement of the Twist-3 ETQS function for gluons through A_N for inclusive jets. Figure 3-6 shows the expected error bars for this measurement after analyzing RHIC Run 17 data. Again, the statistical errors would be reduced by a factor of two with the additional data from a 10 week 1.1 fb^{-1} 500 GeV run.

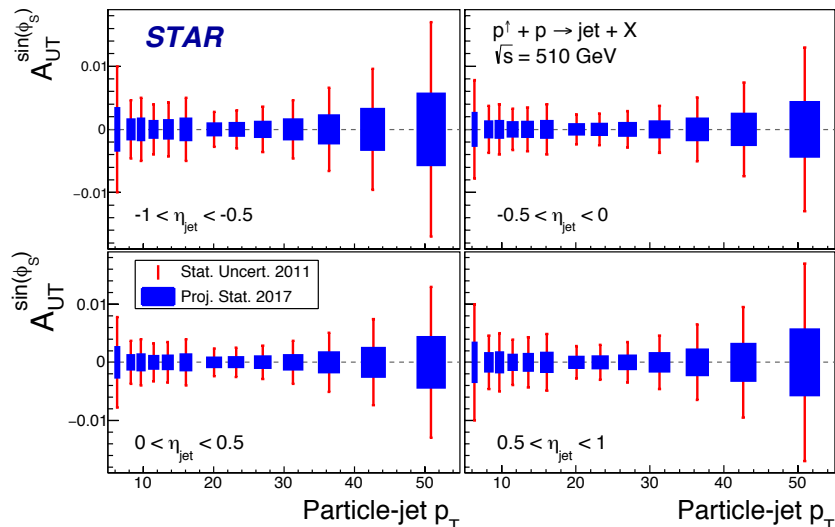


Figure 3-6 The statistical uncertainties for $A_{UT}^{\sin(\phi_s)}$ sensitive to the Twist-3 ETQS function for gluons, as function of particle-jet p_T for 4 bins in rapidity measured in STAR for transversely polarized p+p collisions at 500 GeV (Run-2011 + Run-2017)

3.2 Physics opportunities with (un)polarized proton-Nucleus collisions

In spite of the remarkable phenomenological successes of QCD, a quantitative understanding of the hadronization process is still one of the great challenges for the theory. Hadronization describes the transition of a quark or gluon into a final state hadron. It is a poorly understood process even in elementary collisions. RHIC's unique versatility will make it possible to study hadronization in vacuum and in the nuclear medium, and additionally with polarized beams.

It has long been recognized that the hadron distributions within jets produced in p+p collisions are closely related to the fragmentation functions that have typically been measured in e^+e^- collisions and SIDIS. The key feature of this type of observable is the possibility to determine the relevant momentum fraction z experimentally as the ratio of the hadron to the jet transverse momentum. But only within the past year [26] has the quantitative relationship been derived in a form that enables measurements of identified hadrons in jets in p+p collisions to be included in fragmentation function fits on an equal footing with e^+e^- and SIDIS data. Furthermore, hadrons in p+p jets provide unique access to the gluon fragmentation function, which is poorly determined in current fits [27], in part due to some tension found in the inclusive high p_T pion yields measured by the PHENIX and ALICE collaborations. Here, the proposed measurements can provide valuable new insight into the nature of this discrepancy. It is specifically noted that p+p and p+A collisions provide the ideal tool to study gluon fragmentation. In Deep Inelastic Scattering (DIS) the

fragmentation of gluons cannot be accessed directly as even in processes as photon gluon fusion and charm production, which tag on gluon initiated processes, the parton fragmenting is a quark not a gluon. Gluon fragmentation in DIS can only be studied in higher order processes, i.e. 3 jet events or through the evolution.

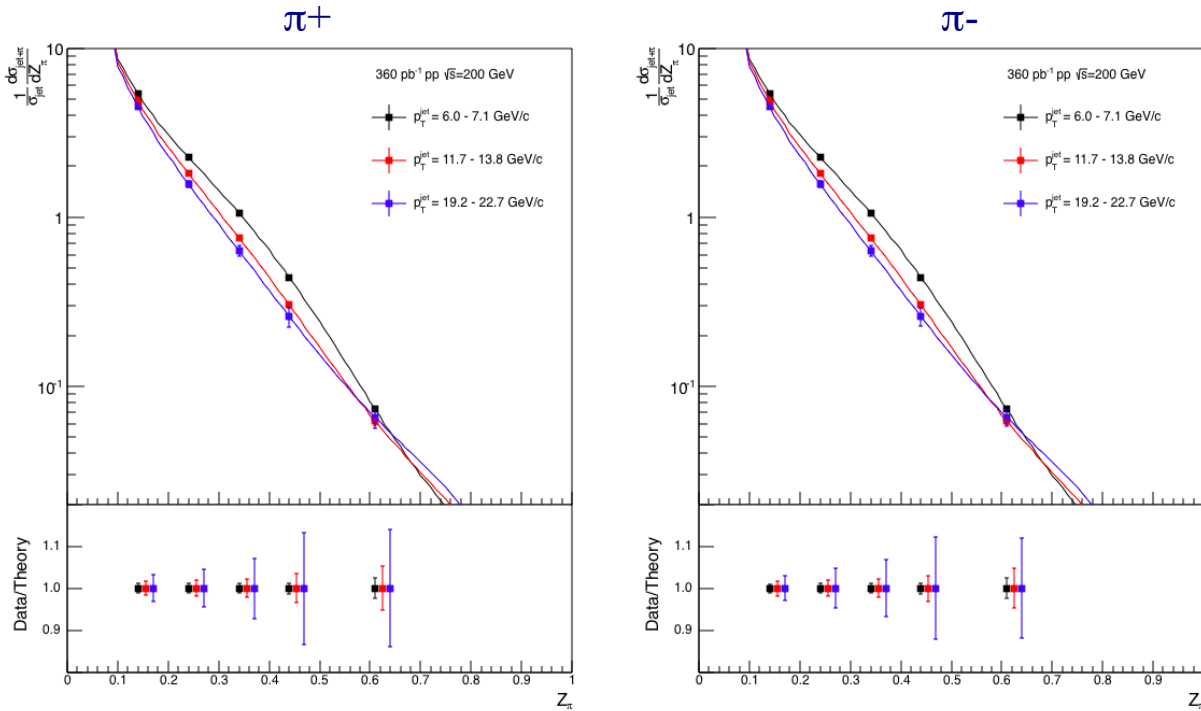


Figure 3-7: Anticipated precision for identified pions within jets at $|\eta| < 0.4$ in 200 GeV p+p collisions for three representative jet p_T bins. The data points are plotted on theoretical predictions based on the DSS14 pion fragmentation functions [26,27]. Kaons and (anti)protons will also be measured, over the range from $z < 0.5$ at low jet p_T to $z < 0.2$ at high jet p_T , with uncertainties a factor of ~ 3 larger than those for pions.

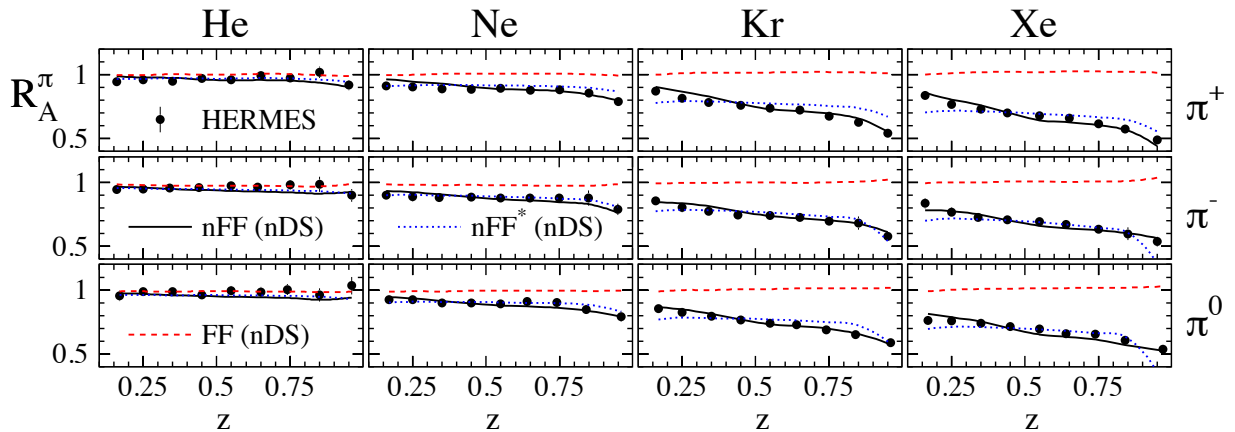


Figure 3-8: R_{eA} in SIDIS for different nuclei in bins of z as measured by HERMES [Error! Bookmark not defined.]. The solid lines correspond to the results using effective nuclear FF [28] and the nDS medium modified parton densities [29]. The red dashed lines are estimates assuming the nDS medium modified PDFs but standard DSS vacuum FFs [30] and indicate that nPDFs are insufficient to explain the data

This development motivated STAR to initiate a program of identified particle fragmentation function measurements using p+p jet data at 200 and 500 GeV from 2011, 2012, and 2015. Figure 3-7 shows the precision that is anticipated for identified π^+ and π^- in 200 GeV p+p

collisions for three representative jet p_T bins after the existing data from 2012 and 2015 are combined with future 200 GeV p+p data from 2023. Identified kaon and (anti)proton yields will also be obtained, with somewhat less precision, over a more limited range of hadron z . Following Run-2017, the uncertainties for 500 GeV p+p collisions will be comparable to that shown in Figure 3-7 at high jet p_T , and a factor of ~ 2 larger than shown in Figure 3-7 at low jet p_T . Identified hadron yields will also be measured multi-dimensionally vs. j_T , z , and jet p_T , which will provide important input for unpolarized TMD fits.

Data from the HERMES experiment [31] have shown that production rates of identified hadrons in semi-inclusive deep inelastic $e+A$ scattering differ from those in $e+p$ scattering. These differences cannot be explained by nuclear PDFs, as nuclear effects of strong interactions in the initial state should cancel in this observable. Only the inclusion of nuclear effects in the hadronization process allows theory to reproduce all of the dependencies (z , x , and Q^2) of R_{eA} seen in SIDIS, as shown in Figure 3-8.

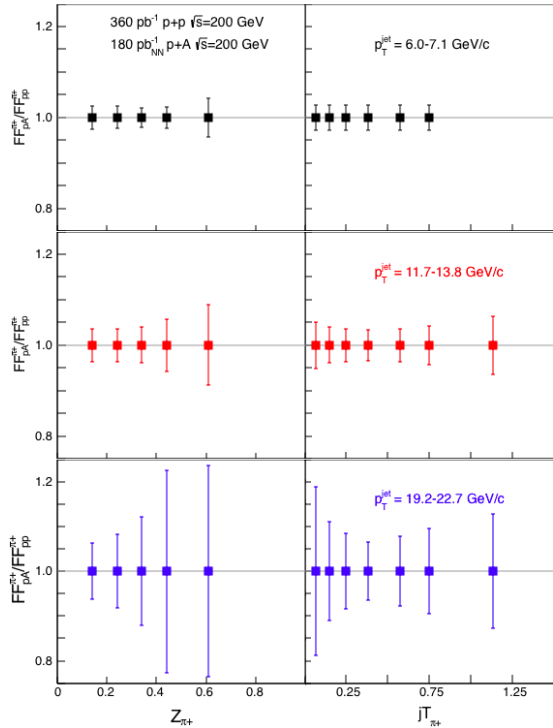


Figure 3-9: Anticipated precision for measurements of π^+ fragmentation functions in p+A/p+p at $|\eta| < 0.4$ vs. z and j_T in 2023 for three representative jet p_T bins. Uncertainties for π^- will be similar to those shown here for π^+ , while those for kaons and (anti)protons will be a factor of ~ 3 larger. Comparable precision is expected for p+Au and p+Al collision systems.

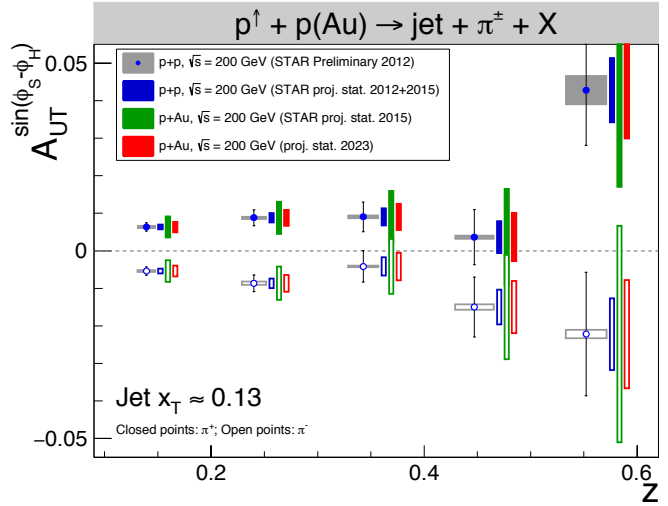


Figure 3-10: Anticipated uncertainties for Collins effect measurements in p+p and p+A at $\sqrt{s_{NN}} = 200$ GeV for $0 < \eta < 1$. All points are plotted at the preliminary values found by STAR for data recorded during 2012. Similar precision will be obtained for p+Au and p+Al during the 2023 run.

It is critical to see if these hadronization effects in cold nuclear matter persist at the higher \sqrt{s} and Q^2 accessed at RHIC and EIC – both to probe the underlying mechanism, which is not understood currently, and to explore its possible universality. The combination of p+p jet data from RHIC and future SIDIS data from EIC will also provide a much clearer picture of modified gluon hadronization than will be possible with EIC data alone. Using the 200 GeV p+Au data collected in 2015, STAR will be able to make a first opportunistic measurement of these hadron-jet

fragmentation functions in nuclei, but the precision will be limited. Additional data will be needed in 2023 in order to provide a sensitive test for universality, as shown in Figure 3-9. Unfortunately, almost no suitable p+Al data were recorded during 2015. Thus, it will also be critical to collect data with a lighter nuclear target in 2023, such as Al, to establish the nuclear dependence of possible medium modifications in the final state, which is not predicted by current models.

STAR has provided the first ever observation of the Collins effect in p+p collisions. RHIC has the unique opportunity to extend the Collins effect measurements to nuclei, thereby exploring the spin-dependence of the hadronization process in cold nuclear matter. This will shed additional light on the mechanism that underlies modified nuclear hadronization. STAR collected a proof-of-principle set of transversely polarized p+Au data during Run-2015. While these data should provide a first estimate of the size of medium-induced effects, a high statistics polarized p+Au dataset and a scan in A is essential to precisely determine the mass dependence of these effects. Figure 3-10 shows the anticipated precision for p+Au and p+Al during the 2023 RHIC run.

It's important to note that all of the measurements discussed in this subsection involve jet detection at mid-rapidity. As such, they don't require forward upgrades to either STAR or sPHENIX. However, they do require good particle identification over quite a wide momentum range, such as that achieved by combining dE/dx and TOF measurements in STAR. If higher precision particle identification can be achieved, as is anticipated with the addition of the iTPC to STAR, the fragmentation function uncertainties will be further reduced, especially for kaons.

Summary of the pp and pA measurements:

Table 3-1 summarizes the pp and pA scientific goals and measurements critical to reach these goals as discussed in the prior chapters. In addition the needed integrated luminosity as well as the detector components critical for the observable are listed.

	Year	\sqrt{s} (GeV)	Delivered Luminosity	Scientific Goals	Observable	Unique STAR Detector Feature
Scheduled RHIC running	2023	p [↑] p @ 200	300 pb ⁻¹ 8 weeks	evolution of ETQS fct. properties and nature of the diffractive exchange in p+p collisions.	A_N for γ A_N for diffractive events	
	2023	p [↑] Au @ 200	1.8 pb ⁻¹ 8 weeks	Nuclear dependence of TMDs and nFF	$A_{UT}^{\sin(\phi_s-\phi_h)}$ modulations of h^\pm in jets, nuclear FF	Particle ID for π, K, p
	2023	p [↑] Al @ 200	12.6 pb ⁻¹ 8 weeks	A-dependence of TMDs and nFF	$A_{UT}^{\sin(\phi_s-\phi_h)}$ modulations of h^\pm in jets, nuclear FF	Particle ID for π, K, p
Potential running	2021	p [↑] p @ 510	1.1 fb ⁻¹ 10 weeks	TMDs at low and high x quantitative comparisons of the validity and the limits of factorization and universality in lepton-proton and proton-proton collisions	A_{UT} for Collins observables, i.e. hadron in jet modulations at $\eta > 1$ and mid-rapidity observables as in 2017 run	

Table 3-1: Summary of the pp and pA measurements as planned in the years 2021 to 2023 using the existing STAR detector as of 2021 for $-1 < \eta < 2$.

3.3 Physics opportunities with Nucleus-Nucleus collisions

In 2020+, with the iTPC upgrade, the STAR experiment will be in an excellent position to measure di-electrons in Au+Au collisions at $\sqrt{s_{NN}} = 200$ GeV with unprecedented precision. In addition, the hypertriton lifetime measurements will be improved very significantly and may have important implications on astrophysics. Below we demonstrate these two physics cases in detail.

3.3.1 Di-electron Mass Spectrum Measurement in 2020+

Ultra-relativistic heavy ion collisions provide a unique environment to study the properties of strongly interacting matter at high temperature and high energy density. Leptons and photons are penetrating probes of the hot, dense medium since they are not affected by the strong interaction and therefore they can probe the whole evolution of the collision.

In the low invariant mass range of produced lepton pairs ($M_{\mu} < 1.1$ GeV/c²), we can study vector meson in-medium properties through their di-lepton decays, where modifications of mass and width of the spectral functions observed may relate to the possibility of chiral symmetry restoration [32, 33]. The di-lepton spectra in the intermediate mass range ($1.1 < M_{\mu} < 3.0$ GeV/c²) are directly related to thermal radiation of the Quark-Gluon Plasma (QGP) [32,33]. However, contributions from other sources have to be obtained. Such contributions include background pairs from correlated open heavy flavor decays ($c\bar{c} \rightarrow l^+l^-X$ or $b\bar{b} \rightarrow l^+l^-X$). In addition, photons in the low transverse momentum range $1 < p_T < 4$ GeV/c are used to study thermal radiation from QGP and hadronic gas.

It is found that a broadened ρ spectral function [34], which describes SPS di-lepton data, consistently accounts for the STAR low mass di-electron excess in Au+Au collisions at $\sqrt{s_{NN}} = 19.6, 27, 39, 62.4,$ and 200 GeV [35, 36, 37, 38, 39, 40]. In addition, with the total baryon density nearly a constant and the di-lepton emission rate dominant in the critical temperature region at $\sqrt{s_{NN}} = 17.3-200$ GeV, the excess di-lepton yields in the low mass region, normalized to the charged particle multiplicity at mid-rapidity, are found to be proportional to the calculated lifetimes of the medium [40]. The models with the same physics ingredients also describe the direct virtual photon production at $1 < p_T < 3$ GeV/c measured by STAR [41].

The iTPC upgrade will reduce the systematic uncertainties on hadron contamination, efficiency correction, acceptance differences between unlike-sign and like-sign pairs, and cocktail subtraction for di-electron measurement. This will result in a factor of two reductions in the systematic uncertainties of di-electron excess yields. In addition, the iTPC will enlarge the acceptance for di-electron measurement by more than a factor of two in the low mass region, which will reduce the statistical uncertainties by more than a factor of $\sqrt{2}$. This improvement is necessary for our fundamental understanding of hot QCD matter.

With the iTPC upgrade, the future measurements from the Beam Energy Scan Phase II at RHIC, will map out the dependence of modified ρ spectral function on the total baryon density in Au+ Au collisions at $\sqrt{s_{NN}} = 7.7-19.6$ GeV. In addition, the iTPC upgrade will enable a much more precise measurement of di-electron mass spectra in $\sqrt{s_{NN}} = 200$ GeV Au+Au collisions, which is necessary for us to connect the experimental observables to chiral symmetry restoration. In the vacuum, chiral symmetry is spontaneously broken, which results in mass differences between chiral partners [e.g. ρ and a_1 (1260)]. In the hot, dense medium, chiral symmetry is expected to restore and the mass distributions of ρ and a_1 (1260) are expected to change and degenerate. Since it is extremely challenging to measure a spectral function for the a_1 (1260) meson, one cannot directly observe the disappearance of the mass splitting between the ρ and a_1 (1260) experimentally. Using the broadened ρ spectral function, QCD and Weinberg sum rules, and inputs

from Lattice QCD, theorists have demonstrated that when the temperature reaches 170 MeV, the derived ρ (1260) spectral function is the same as the in-medium ρ spectral function, a signature of chiral symmetry restoration [42]. The Lattice QCD calculations on the order parameters are only valid at low baryon chemical potential ($\mu_B \sim 0$). A precise measurement of di-lepton mass spectra at $\mu_B \sim 0$ is needed for theorists to constrain the broadened ρ spectral function used in the model calculations and to establish the connection between experimental di-lepton observables and chiral symmetry restoration.

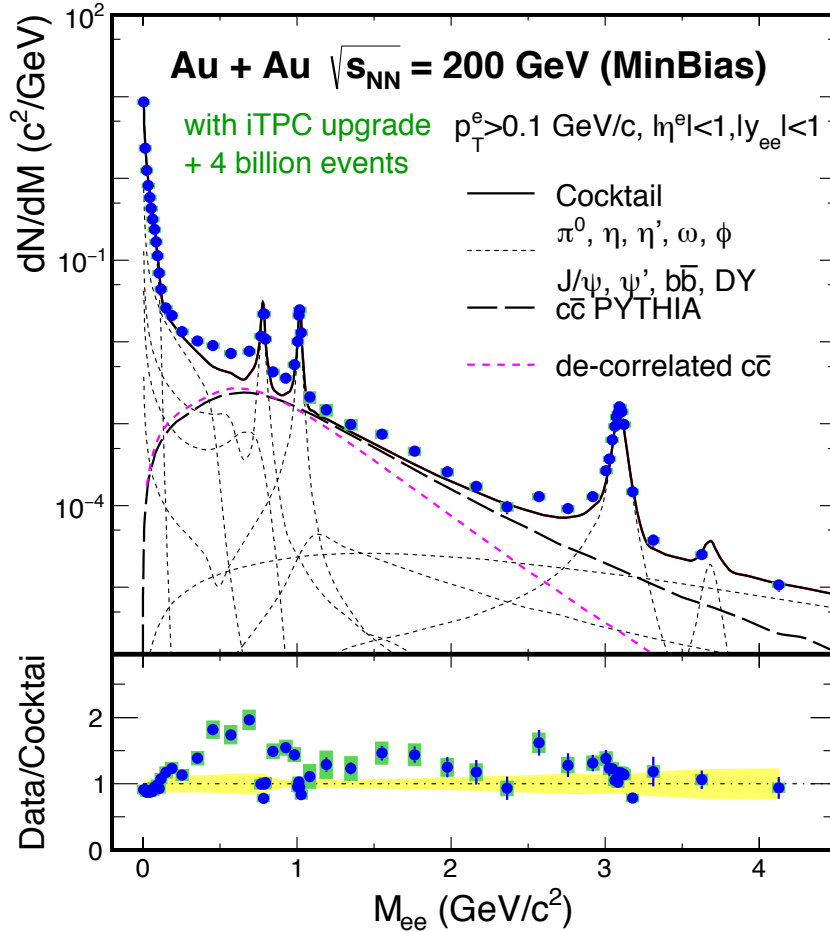


Figure 3-11: The precision projection of invariant mass spectrum in the STAR acceptance ($p_t^e > 0.1$ GeV/c, $|\eta_e| < 1$, and $|y_{ee}| < 1$) from four billion $\sqrt{s_{NN}} = 200$ GeV Au+Au minimum-bias collisions with the iTPC upgrade. The mass spectrum is compared to the hadronic cocktail simulations without the vacuum ρ contribution. The vertical bars on data points depict the statistical uncertainties, while the systematic uncertainties are shown as green boxes. Yellow bands in the bottom panels depict the systematic uncertainties on the cocktail. The dashed line indicates the charm decay di-electron contribution from Pythia calculations scaled with N_{bin} . The magenta dashed line represents the charm decay di-electron contribution if c and $c\bar{c}$ are fully de-correlated.

Figure 3-11 shows the precision projection of invariant mass spectrum in the STAR acceptance ($p_t^e > 0.1$ GeV/c, $|\eta_e| < 1$, and $|y_{ee}| < 1$) from four billion $\sqrt{s_{NN}} = 200$ GeV Au+Au minimum-bias collisions with the iTPC upgrade. With this improvement, we will be able to distinguish models with different ρ -meson broadening mechanisms, for example, Parton-Hadron String Dynamic (PHSD) transport model [43] versus Rapp's microscopic many-body model with macroscopic medium evolution [44], as shown in Figure 3-12.

In the intermediate mass region, the future improved measurement will enable us to obtain the very important information from the QGP thermal radiation. The improve measurements will enable us to see a possible difference between the inclusive di-electron measurement and the cocktail in which the charm decay di-electron contribution from PYTHIA calculations, scaled with N_{bin} , is used. The PYTHIA case serves as an upper limit of the charm decay background for the QGP thermal radiation. If the c and \bar{c} correlation were fully broken due to interactions with the medium, the charm decayed di-electron contribution would become much less compared to the inclusive di-electron signal, as illustrated by the magenta dashed curve in Figure 3-11.

Experimentally, the challenging analysis on charmed decayed di-electron is ongoing from the data sets taken with the Heavy Flavor Tracker at STAR. However, the heavy quark dynamics in the medium is under active investigations and will be much better understood by 2020+. Thus the measurement from QGP thermal radiation will become possible with rigorous theoretical efforts and improved di-electron measurements.

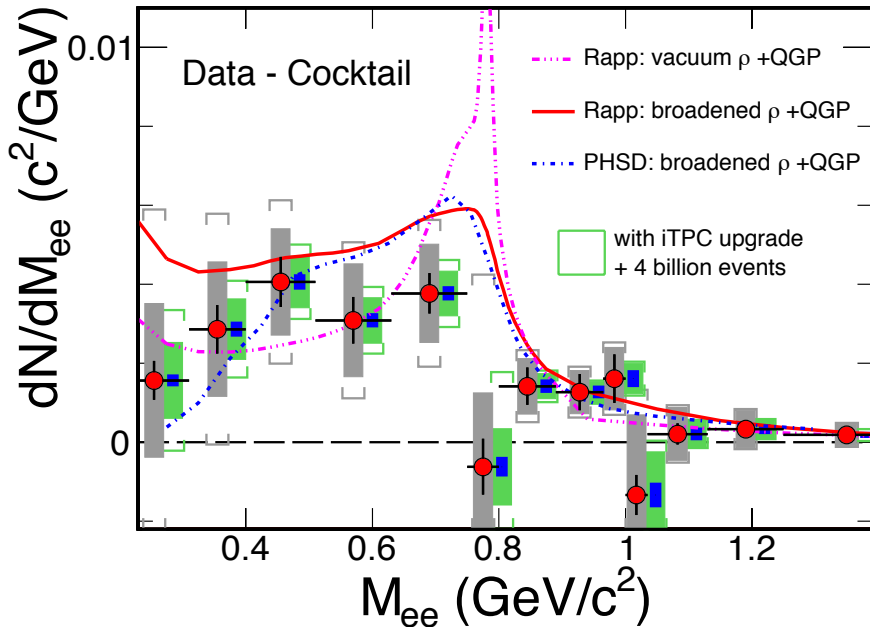


Figure 3-12: The expected statistical and systematic uncertainties of di-electron excess mass spectrum with the iTPC upgrade compared to the current TPC case. The data are from our measurements in $\sqrt{s_{NN}} = 200 \text{ GeV}$ Au+Au collisions [38]. Model comparisons are also shown. The boxes represent systematic uncertainties from data and the brackets represent the total systematic uncertainties including those from cocktails. The grey ones are for the current case while the green ones are for the expected case with the iTPC upgrade. The blue bands represent statistical uncertainties from four billion minimum-bias events with the iTPC upgrade.

3.3.2 Hypertriton Lifetime Measurement in 2020+

The strangeness sector of baryon interactions are key to investigate the possibility of exotic states, the structures of hypernuclear states, and the properties of the core of neutron stars. Depending on the strength of the Hyperon-Nucleon (YN) interaction, the collapsed stellar core of a neutron star could consist of hyperons, strange quark matter, or a kaon condensate [45]. Recent astrophysical observation on large mass of neutron stars [46,47] raised question on the conventional understanding of the equation of state (EOS) of neutron star, the so-called hyperon puzzle. The onset of hyperon in the core of neutron stars and the consequent softening of the EOS would result in a small value of neutron star mass. Quantum MC calculations find that stronger constraints on the hyperon-neutron force are necessary in order to properly access the role of hyperons in neutron stars [48].

From experimental side, the lifetime of a hypernucleus depends on the strength of the YN interaction. Therefore, a precise determination of the lifetime of hypernuclei provides direct information on the YN interaction strength [49]. Recently measurements in heavy-ion experiments indicate that a hypertriton has a shorter lifetime than a free Lambda [49, 50, 51]. Theoretical interpretations are missed yet. The discrepancy between heavy-ion experimental results and theoretical calculations poses a major problem for the understanding of hypertriton. More work is necessary to understand the physics inside [52].

With upgrades scheduled in STAR, a precise measurement of hypertriton lifetime is expected. The combined statistical and systematic uncertainties for the current lifetime measurement are 30% while the future measurement from four billion minimum-bias Au+Au collisions at $\sqrt{s_{NN}} = 200$ GeV would have 9% combined statistical and systematic uncertainties. Physics implication on interaction strength between Y-N will thus be obtained.

3.4 Physics opportunities with Diffractive and Ultra-Peripheral Collisions in pp, pA and AA

In the past year many new physics opportunities have been discussed for diffractive and Ultra-Peripheral Collisions (UPC) in pp, pA and AA. Different final states, i.e. di-jets and vector mesons can be used to study different questions as listed here.

- The study of wigner functions describing the momentum and spatial structure of gluon in the proton through UPC di-jet production [53].
- The search for glueballs in central exclusive production
- R_{pA} for diffractive di-jets to study the physics of high gluon densities at low x in nuclei
→ Saturation in nuclei
- The spatial structure of nucleons and nuclei for exclusive J/ψ production in ultra-peripheral pp, pA and AA collisions
 - Study unintegrated gluon distribution in nuclei for exclusive J/ψ production in ultra-peripheral pp, pA and AA collisions
 - A first look to the GPD E_g through the measurement of A_{UT} for exclusive J/ψ production in ultra-peripheral $p \uparrow p$ and $p \uparrow A$ collisions

As many of these ideas are new this chapter is in flux and will in the following weeks be replaced by studies detailing the physics opportunities of such a program with STAR. STAR, with RHIC's polarized proton beams, and its Roman Pots (RPs) to tag the forward scattered protons, plus our large jet acceptance - $1 < \eta < 2$ now and - $1 < \eta < 4$ after the forward upgrade, will be uniquely equipped to study phenomena in diffraction and UPC. For many observables, the rapidity gap method and the tagging of the forward scattered proton in the STAR RPs can be realized. The RPs and the ZDC together provide also an excellent experimental opportunity on the one hand to veto the nucleus or proton breaking up and on the other hand to tag on single diffractive processes.

4 Bibliography

- [1] “The STAR Forward Calorimeter System and Forward Tracking System beyond BES-II” Proposal <https://drupal.star.bnl.gov/STAR/starnotes/public/sn0648>
- [2] STAR Collaboration Beam Use Request for run 18 and run 19 <https://drupal.star.bnl.gov/STAR/starnotes/public/sn0670>
- [3] F. Yuan, Phys. Rev. Lett. 100 (2008) 032003; Phys.Rev.D77 (2008) 074019.
- [4] U. D’Alesio, F. Murgia, and C. Pisano, Phys. Rev. D 83 (2011) 034021.
- [5] A. Bacchetta and M. Radici, Phys. Rev. D70 (2004) 094032.
- [6] J. Ralston and D.Soper, Nucl. Phys. B152 (1979) 109.
- [7] R. Jaffe and X. Ji, Nucl. Phys. B375 (1992) 527.
- [8] P. Mulders and R. Tangerman, Nucl. Phys. B461 (1996) 197.
- [9] D. Sivers, Nuovo Cim. C035N2 (2012) 171
- [10] R. L. Jaffe and X. Ji, Phys. Rev. Lett. 67 (1991) 552.
- [11] C. Collins, Nucl. Phys. B396 (1993) 161
- [12] C. Collins, S. F. Heppelmann, and G. A. Ladinsky, Nucl. Phys. B420 (1994) 565.
- [13] A. Airapetian *et al.* (HERMES Collaboration), Phys. Rev. Lett.94 (2005) 012002; 103 (2009) 152002; Phys. Lett. B693 (2010) 11.
- [14] V. Y. Alexakhin *et al.* (COMPASS Collaboration), Phys. Rev. Lett. 94 (2005) 202002; E. S. Ageev *et al.* (COMPASS Collaboration), Nucl. Phys. B765 (2007) 31; M. G. Alekseev *et al.* (COMPASS Collaboration), Phys. Lett. B673 (2009) 127; B692 (2010) 240; C. Adolph *et al.* (COMPASS Collaboration), Phys. Lett. B717, 376 (2012); N. Makke (COMPASS Collaboration), PoS EPS-HEP2013 (2013) 443.
- [15] A. Airapetian *et al.* (HERMES Collaboration), JHEP 0806 (2008) 017.
- [16] C. Adolph *et al.* (COMPASS Collaboration), Phys. Lett. B 713 (2012) 10.
- [17] R. Seidl *et al.* (Belle Collaboration), Phys. Rev. Lett 96 (2006) 232002; Phys. Rev. D 86 (2012) 039905(E).
- [18] A. Vossen *et al.* (Belle Collaboration), Phys. Rev. Lett. 107 (2011) 072004.
- [19] STAR Collaboration, Phys.Rev.Lett. 115 (2015) 242501
- [20] S. Pisano and M. Radici, Eur. Phys. J. A52 (2016) no.6, 155
- [21] Z.-B. Kang, Phys. Rev. D83 (2011) 036006.
- [22] M. Anselmino *et. al.*, Phys.Rev. D73 (2006) 014020.
- [23] STAR Collaboration, submitted to PRL (2015), arXiv:1511.06003.
- [24] P. Sun, J. Isaacson, C.-P.Yuan and F. Yuan arXiv:1406.3073.
- [25] A. V. Efremov and O. V. Teryaev, Sov. J. Nucl. Phys. 36 (1982) 140 [Yad. Fiz. 36, 242 (1982)]; Phys. Lett. B 150 (1985) 383
J.-W. Qiu and G. F. Sterman, Phys. Rev. Lett. 67 (1991) 2264; Nucl. Phys. B 378 (1992) 52; Phys. Rev. D 59 (1999) 014004.
- [26] T. Kaufmann, A. Mukherjee, and W. Vogelsang, Phys.Rev. D92 (2015) 5, 054015.
- [27] D. de Florian, R.Sassot, M.Epele, R.J.Hernandez-Pinto, and M.Stratmann, Phys.Rev. D91 (2015) 1, 014035
- [28] R. Sassot, M. Stratmann, and P. Zurita, Phys. Rev. D81 (2010) 054001.
- [29] D. de Florian and R. Sassot, Phys. Rev. D 69 (2004) 074028.
- [30] D. de Florian, R. Sassot, and M. Stratmann, Phys. Rev. D 75, 114010 (2007); D 76, 074033 (2007).
- [31] A. Airapetian *et al.* (HERMES Collaboration), Phys. Lett, B577 (2003) 37; Nucl. Phys. B780 (2007) 1; Phys. Lett. B684 (2010) 114.
- [32] R. Rapp and J. Wambach, Adv. Nucl. Phys. 25, 1 (2000).
- [33] G. David, R. Rapp and Z. Xu, Phys. Rept. 462, 176 (2008).
- [34] R. Rapp, J. Wambach, and H. van Hees, arXiv:0901.3289
- [35] D. Adamova *et al.*, Phys. Rev. Lett. 91, 042301 (2003); G. Agakichiev *et al.*, Eur. Phys. J. C 41, 475 (2005); D. Adamova *et al.*, Phys. Lett. B 666, 425 (2008).
- [36] R. Arnaldi *et al.*, Phys. Rev. Lett. 96, 162302 (2006); R. Arnaldi *et al.*, Phys. Rev. Lett. 100, 022302 (2008); R. Arnaldi *et al.*, Eur. Phys. J. C 59, 607 (2009).

-
- [37] L. Adamczyk et al., Phys. Rev. Lett. 113, 022301 (2014), Erratum-ibid. 113, 049903 (2014).
[38] L. Adamczyk et al., Phys. Rev. C 92, 024912 (2015).
[39] A. Adare et al., Phys. Rev. C 93, 014904 (2016).
[40] L. Adamczyk et al., Phys. Lett. B 750, 64 (2015).
[41] L. Adamczyk et al., Phys. Lett. B 770, 451 (2017).
[42] P.M. Hohler and R. Rapp, Phys. Lett. B 731, 103 (2014).
[43] O. Linnyk et al., Phys. Rev. C 85, 024910 (2012).
[44] R. Rapp, PoS CPOD2013, 008 (2013); R. Rapp, private communications.
[45] J.M. Lattimer and M. Prakash, Science 304, 536 (2004)
[46] P.B.Demorest, T.Pennucci, S.M.Ransom, M.S.E.Roberts and J.W.T.Hessels, Nature 467, 1081 (2010)
[47] J. Antoniadis et al., Science 340, 1233232 (2013)
[48] D. Lonardonì, A. Lovato, S. Gandolfi and F. Pederiva, Phys. Rev. Lett. 114, 092301 (2015)
[49] The STAR Collaboration, Science 328, 58 (2010)
[50] C. Rappold et al., Nucl. Phys. A 913, 170 (2013)
[51] The ALICE Collaboration, Phys. Lett. B 754, 360 (2016)
[52] A. Cal, E.V. Hungerford and D.J. Millener, Rev. of Mod. Phys. 88, 035004 (2016)
[53] Y. Hagiwara, Y. Hatta, R. Pasechnik, M. Tasevsky and O. Teryaev, arXiv:1706.01765